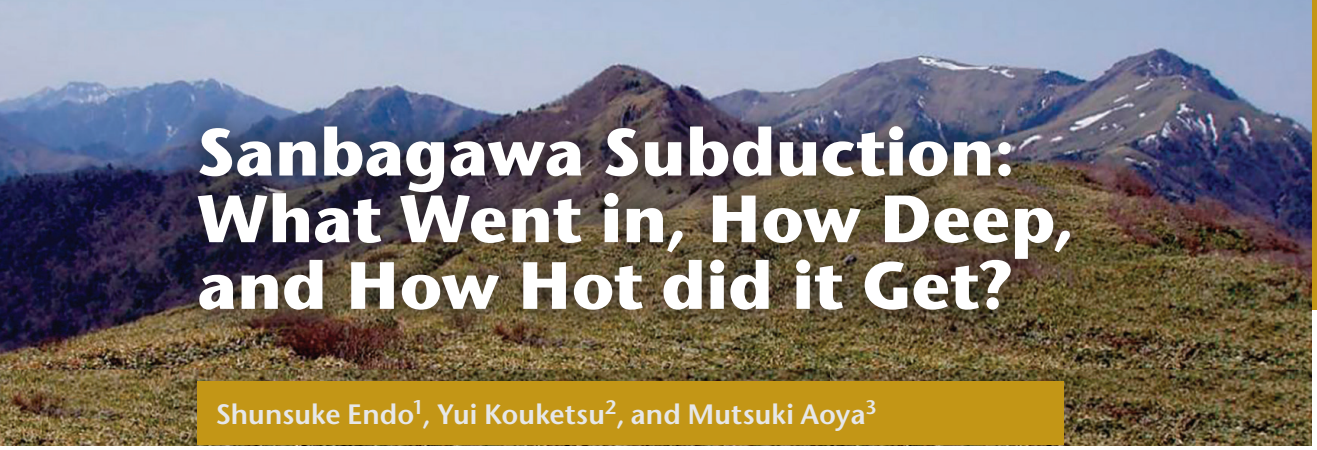

Sanbagawa Subduction: What Went in, How Deep, and How Hot did it Get?

Shunsuke Endo[1], Yui Kouketsu[2], and Mutsuki Aoya[3]

Sasagamine range (Shikoku Mountains) in early spring. The range is made up of a thick metabasalt layer, a prominent feature of the Sanbagawa belt in central Shikoku. Photo: Mutsuki Aoya.

1811-5209/24/0020-077$2.50 DOI: 10.2138/gselements.20.2.77

The Sanbagawa belt is a "coherent" oceanic subduction-type metamorphic region representing a rock package predominantly derived from oceanic crust and accreted at depths of 20–80 km (300–700 °C). The thermal structure and lithological layers are complexly deformed but semi-continuous, in contrast to more commonly reported subduction-related domains dominated by mélange. The coeval Shimanto accretionary complex records accretion at depths <15 km and the rocks are primarily terrigenous sediments. The Sanbagawa belt has a greater proportion of mafic rocks than the Shimanto complex, implying progressive peeling-off of oceanic plate stratigraphy with more basaltic oceanic crust slices accreted at deeper levels. Tectonic exhumation can be explained by three separate phases dominated by buoyancy-driven upflow, ductile thinning, and normal faulting.

Keywords: Sanbagawa; oceanic subduction; exhumation; mafic and pelitic schists; Raman spectroscopy

INTRODUCTION

Subduction of oceanic lithosphere is a unique process by which cold near-surface materials enter the mantle. This cycling of rocks, fluids, and volatiles is a fundamental control on the thermal and chemical evolution of the Earth. Oceanic subduction is also the cause of active tectonics forming the ring of circum-Pacific or Cordilleran-type orogens. The exposure of high-pressure (P)/low-temperature (T) metamorphic rocks in such orogenic belts implies that at least a part of the subducted rocks returns to the surface when suitable conditions are met. Characterization of these high-P/T metamorphic rocks from the field-scale to the micro-scale is essential to decipher these ancient records of the deep subduction interface; this information is also important for interpreting geophysical data from modern subduction zones.

The Phanerozoic geology of Japan has developed in the framework of a subduction relay, where multiple discrete oceanic plates follow each other as they move beneath the East Asian margin. As a result, Japan includes many sites suitable for exploring subduction-related processes. The Sanbagawa belt is of particular interest and importance as one of the best-preserved examples of a fossilized subduction interface in the world, comprising a more than 800-km-long occurrence of high-P/T metamorphic rocks, distributed on the south side (footwall side) of the Median Tectonic Line (MTL; Fig. 1A). The most detailed documentation of the lithological structure of the belt is presented in the recent 1:50,000 geological maps of key areas of the Shikoku Mountains (e.g., Aoya et al. 2013; Endo and Yokoyama 2019). Historically, in the 1950s to 70s, these areas were the focus of extensive geological surveys, including both mapping and deep borehole drilling, which were largely motivated by exploration for Besshi-type cupriferous deposits. This work was accompanied and followed by numerous scientific studies utilizing techniques of metamorphic petrology, structural geology, and geochronology (e.g., Wallis and Okudaira 2016). Recent developments in P–T estimation methods (geothermobarometers) using micro-Raman spectroscopy have also improved our understanding of the spatial variation of metamorphic conditions in the Sanbagawa belt. In this study, we review the lithological, metamorphic, and structural architecture of the Sanbagawa belt, incorporating these recent advances, and explore its exhumation history by integrating the available geological data.

WHAT SUBDUCTED

Source Rocks

To the south of the Cretaceous Sanbagawa belt, there are two separate and shallower subduction (accretionary) complexes: the mainly Jurassic Chichibu belt (comprising the Mikabu, Northern-Chichibu, and Southern-Chichibu belts) and the Cretaceous Shimanto belt (Fig. 1A). The dominant source rocks for all three subduction complexes are constituents of typical oceanic-plate stratigraphy. In order from the bottom to top are: basalt, limestone, pelagic cherty sediments, and terrigenous clastic sediments such as mudstone and sandstone. The basaltic basement is mainly composed of mid-ocean ridge basalt (MORB), but can also include various amounts of oceanic island basalt (OIB) that is commonly closely associated with limestone. The age and proportion of these source rocks reflect the nature of the subducted plate at the trench and the later accretion process at depths.

1 Department of Earth Science
Shimane University
Matsue 690-8504, Japan
E-mail: s-endo@riko.shimane-u.ac.jp

2 Graduate School of Environmental Studies
Nagoya University
Nagoya 464-8601, Japan
E-mail: kouketsu.yui@nagoya-u.jp

3 Graduate School of Technology, Industrial and Social Sciences
Tokushima University
Tokushima 770-8506, Japan
E-mail: aoya@tokushima-u.ac.jp

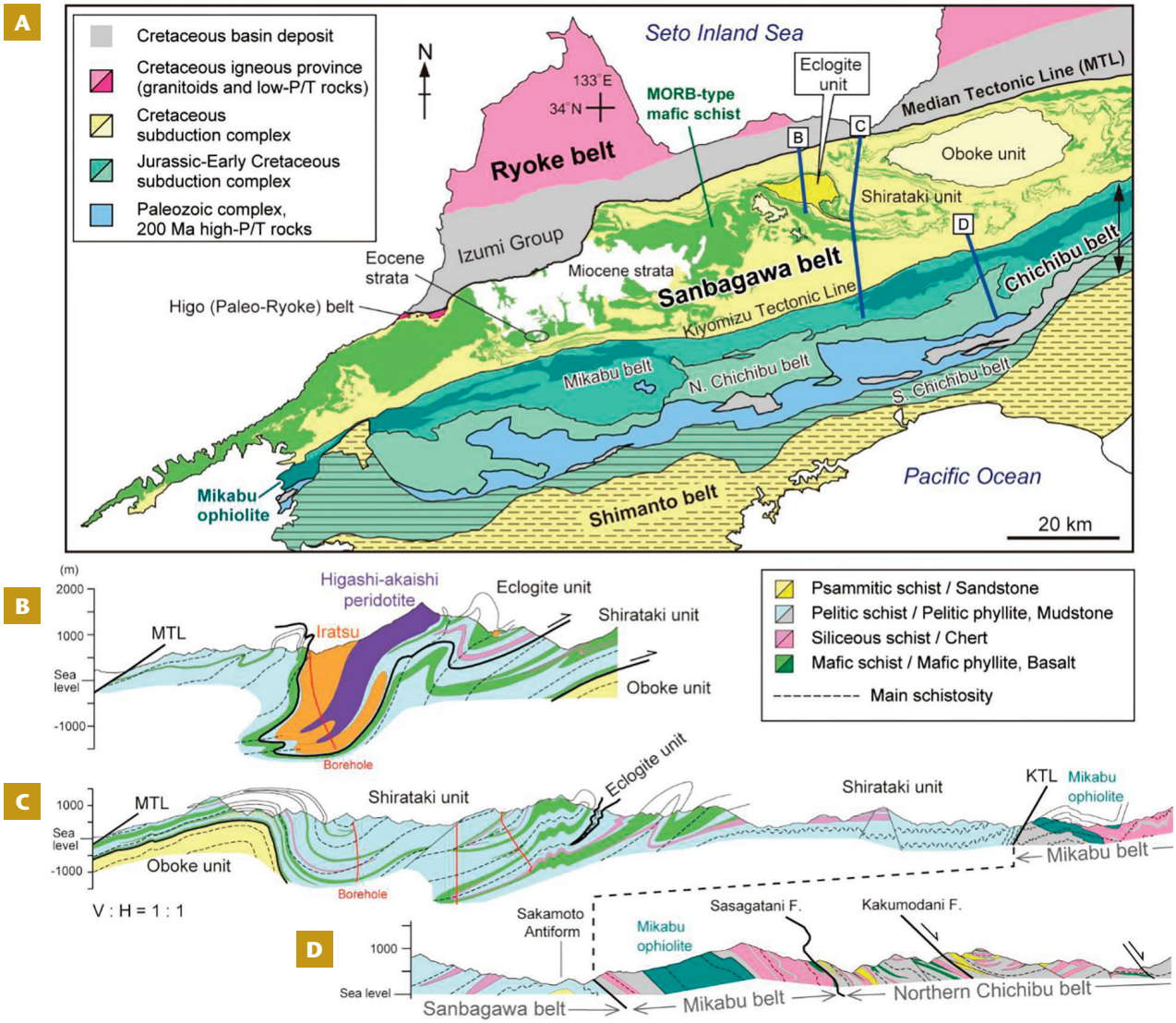

Figure 1 (**A**) Geotectonic division map of Shikoku. Modified after Miyazaki et al. (2016) and Hara et al. (2018). (**B**) Cross section of the Sanbagawa orogenic core. Modified after Aoya et al. (2013). (**C**) Cross section showing the internal structure of the Shirataki unit. Modified after Aoya (2022). (**D**) Cross section showing structural relations through the Sanbagawa, Mikabu, and Northern Chichibu belts. Modified after Endo and Yokoyama (2019).

The Cretaceous Shimanto-Sanbagawa composite belt is structurally overlain by the older Chichibu belt (Fig. 1A, 1D). In contrast to the Chichibu belt, the mafic rocks in the Shimanto and Sanbagawa belts are dominantly MORB and contain few seamount remnants (OIB and limestone). This change in geological characteristics reflects a change in the identity and nature of the subducting plate through time. Reconstructed oceanic-plate stratigraphy suggests an abrupt change in the age of the subducting oceanic plate during the middle Cretaceous (e.g., Ueda and Miyashita 2005). Subsequently, differences in the ages of MORB units and overlying terrigenous sediment in the Late Cretaceous subduction complexes progressively decrease with time, marking the approach of the Izanagi-Pacific ridge towards the East Asia trench, finally arriving around 50 ± 10 Ma (e.g., Wu et al. 2022).

One of the characteristics of the Shimanto accretionary complex is the predominance of terrigenous siliciclastic sediments, reflecting an abundant sediment flux during Cretaceous magmatic flare-up events resulting in surface uplift and active erosion of older accretionary complexes and arc magmatic rocks (Hara et al. 2017). In contrast, the contemporaneous but more deeply buried Sanbagawa metamorphic rocks contain larger volumes of MORB-type mafic schist (Fig. 1A), implying progressive peeling of the oceanic crust with subducted depth, and final underplating of basaltic basement slices at depths of >20 km (Endo et al. 2018).

Structural Architecture

The Sanbagawa belt in the Shikoku Mountains consists of three litho-structural units: the Oboke (~75 Ma), Shirataki (95–81 Ma: this unit is also referred to as the Besshi unit), and Eclogite units (~90 Ma with minor ~120–110 Ma domains), in ascending order of structural level (Aoya et al. 2013; Endo et al. 2018; Nagata et al. 2019) (Fig. 1B, 1C). Overall, these units form a stack of underplated tectonic slices (nappe-stacking structure), where the upper structural unit is older and formed deeper than the lower one. Large-scale mafic schist units associated with the Besshi-type copper deposits appear in the upper structural levels of the Shirataki unit. This type of mafic schist originates as Late Jurassic MORB (~150 Ma; Nozaki et al. 2013). Detailed field mapping of the MORB-type mafic schist has revealed

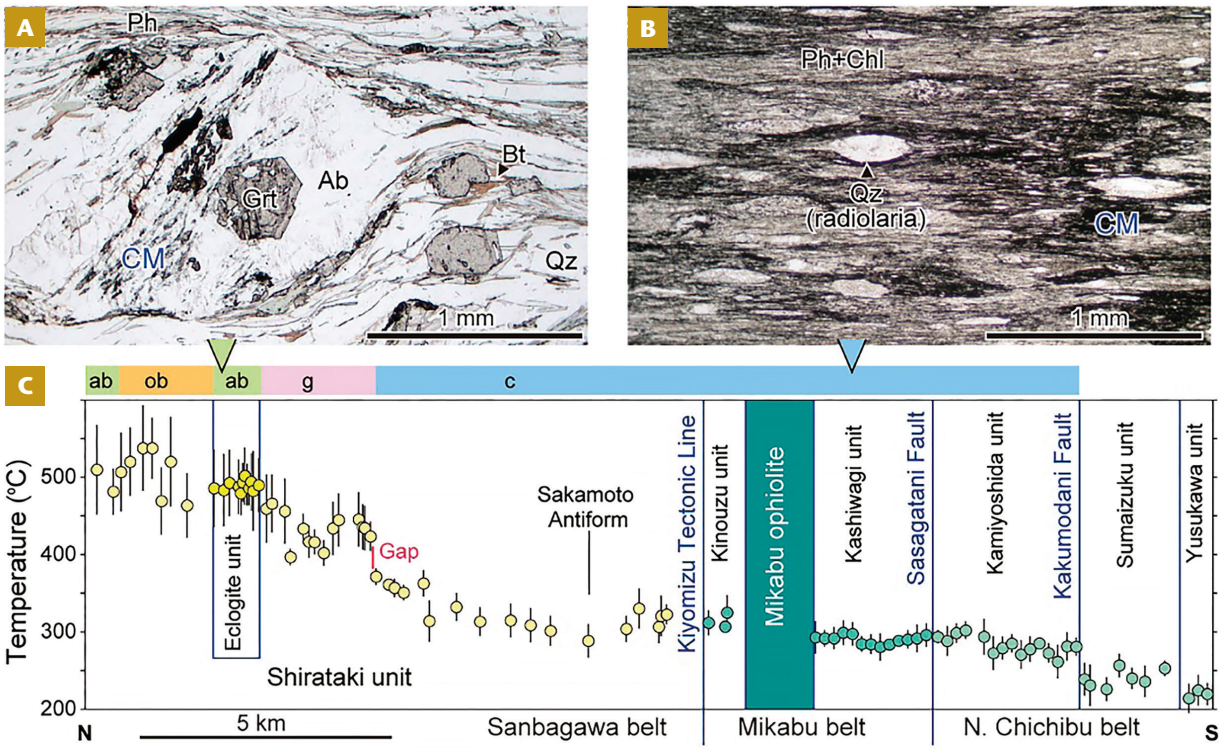

Figure 2 Peak temperatures recorded in samples of pelitic schist. Progressive Sanbgawa metamorphic zones are: chlorite zone (c), garnet zone (g), albite-biotite zone (ab), and oligocalse-biotite zone (ob). (**A, B**) Photomicrographs of pelitic schist consisting of quartz (Qz), albite (Ab), phengite (Ph), chlorite (Chl), and carbonaceous material (CM: blackish parts). Garnet (Grt) and biotite (Bt) appear in the high-temperature zones. (**C**) Peak-temperature profile based on Raman CM geothermometry. Data sources are Kouketsu et al. (2021) for the northern area (Asemigawa route: yellow circles) and Endo and Wallis (2017) for the southern area—results from samples collected close to the line of section D in Figure 1A (green circles).

the tightly folded internal structure of the Shirataki unit (Fig. 1B, 1C). These folds form an "orogenic core" of the belt, comprising the highest-grade Eclogite unit. Locally, the Eclogite unit contains bodies of coarse-grained metabasalt/gabbro, such as the kilometer-scale Iratsu body, but otherwise shows a similar rock association to the Shirataki unit (Fig. 1B). The Iratsu and associated bodies have older protolith ages and preserve older (~120–110 Ma) metamorphic stages than the rest of the belt (e.g., Aoya and Endo 2017). Although the origin and tectonic implications of older stages in the Iratsu body remain controversial, these are certainly key to understanding how the early Sanbagawa subduction system developed.

To the south, the main part of the Sanbagawa belt described above is bounded by the Kiyomizu Tectonic Line (KTL) (Fig. 1A). Locally preserved primary structural relationships suggest that weakly metamorphosed Jurassic to Early Cretaceous accretionary complexes that lie further south (the Mikabu and Northern-Chichibu belts) overlie the Sanbagawa metamorphic rocks (Fig. 1D).

HOW DEEP AND HOW HOT?

Thermal Structure

Higashino (1990), a milestone in metamorphic studies of the Sanbagawa belt, was the first to document the detailed distribution of different metamorphic zones of the Sanbagawa metamorphism in Shikoku Mountains. Based on index minerals in pelitic schist (metamorphosed mudstone; Fig. 2A, 2B), four mineral zones were defined: chlorite, garnet, albite-biotite, and oligoclase-biotite zones, in ascending order of metamorphic grade. As is common in high-P/T orogens, most of the Sanbagawa belt consists of the low-grade chlorite zone. One of the limitations of traditional mineral-zone mapping is the inability to discern any details of the thermal structure within this chlorite zone. The development of Raman carbonaceous material (CM) geothermometry for low-grade metamorphism using the crystallinity of CM (e.g., Kaneki and Kouketsu 2022) has overcome this problem, and has been used to reveal the detailed thermal structure along a traverse across the main part of the Sanbagawa belt (Kouketsu et al. 2021) and into the Northern Chichibu belt (Endo and Wallis 2017) (Fig. 2C). These results clearly show a steep temperature gradient in the orogenic core, although overall, the temperature distribution is semi-continuous. Raman CM profiles can be used in this way to assess the degree to which there is a continuous record of the conditions along the paleo-subduction boundary and the degree to which this has been disrupted by the formation of tectonic discontinuities (Fig. 2C). A combination of Raman studies with lithological and structural mapping suggests the presence of two major litho-structural unit (nappe) boundaries and a second-order tectonic discontinuity close to the boundary between the chlorite and garnet zones (Kouketsu et al. 2021).

Deep Sediment Subduction

The development of "Raman elastic geobarometry" is a second remarkable advance in metamorphic geology. After entrapment of an inclusion by a host mineral at depth, different elastic properties between inclusion and host minerals generate local overpressure or underpressure during exhumation. Residual pressures retained by quartz inclusions in garnet can be detected by micro-Raman spectroscopy, and entrapment P–T conditions can be estimated via elastic modeling (e.g., Kouketsu et al. 2014a; Angel et al. 2017). Applying this method to the Sanbagawa belt (Fig. 3A) showed that the area of eclogite-facies metamorphism in pelitic schist is significantly larger than previously thought. This led to a significant expan-

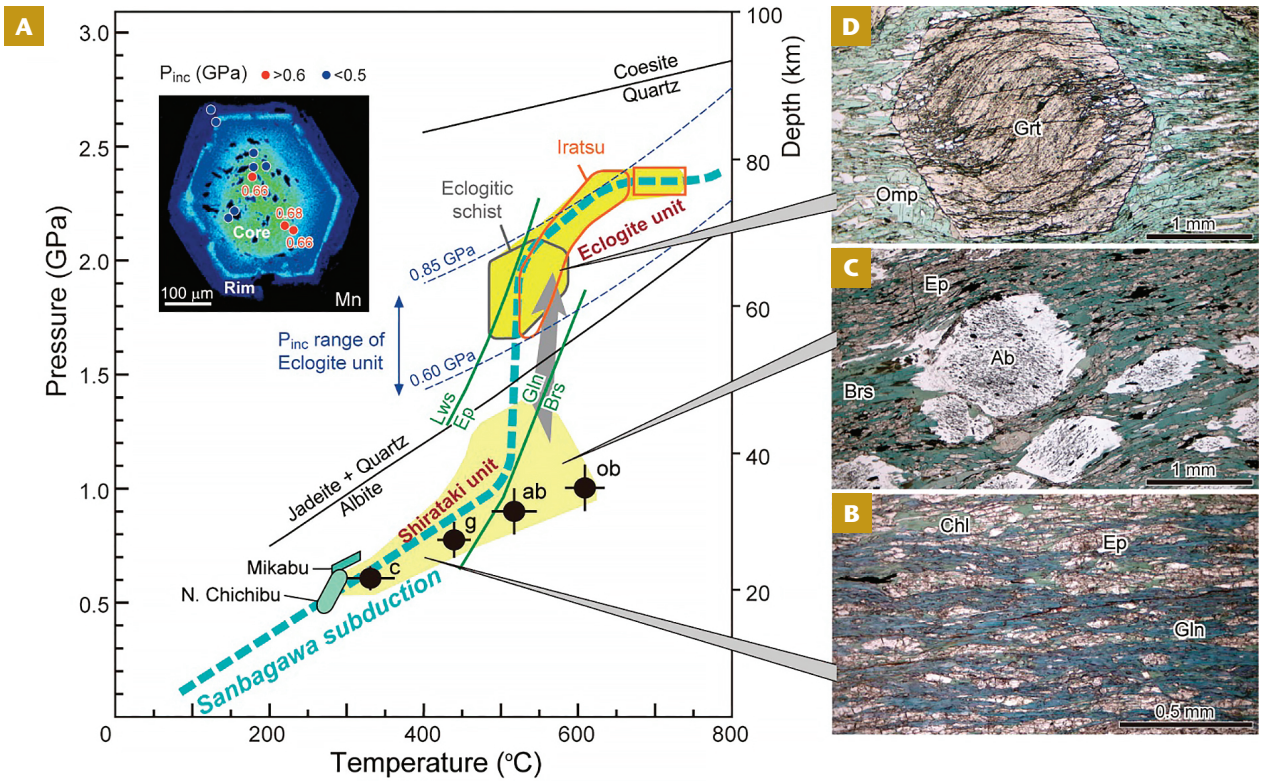

Figure 3 (**A**) Pressure–temperature conditions of the Sanbagawa metamorphism. Modified after Aoya and Endo (2017). Inset image is a Mn compositional map of garnet in pelitic schist from the Eclogite unit, showing residual pressures (P_{inc}) retained by quartz inclusions (Kouketsu et al. 2014b). Lawsonite (Lws)/epidote (Ep) and glaucophane (Gln)/barroisite (Brs) transition curves in mafic rocks (Weller et al. 2015) are also shown. Three photomicrographs (**B**–**D**) show the mineralogical evolution of MORB-type mafic schist. (**B**) Blueschist from a low-grade part (~400 °C) of the Shirataki unit. (**C**) Epidote amphibolite from a high-grade part (~550 °C) of the Shirataki unit. (**D**) Eclogitic schist from the Eclogite unit. Ab = albite, Chl = chlorite, Ep = epidote, Gln = glaucophane, Grt = garnet, Omp = omphacite.

sion of the known extent of the Eclogite unit, implying large volumes of sediment subduction to mantle depths (Kouketsu et al. 2014b). Pelitic schist in the Eclogite unit contains two-stage zoned garnet with an eclogite-facies core and a lower-*P* stage rim (Fig. 3A). Quartz inclusions in the garnet core retain high residual pressures. Detailed surveys of inclusions in the garnet core reveal that paragonite, glaucophane, and rare jadeite were present as Na-rich minerals during eclogite-facies metamorphism of the pelitic schist (Kouketsu et al. 2014b; Taguchi et al. 2019), but in most samples, they subsequently decomposed to form albite porphyroblasts, representing equilibration during post peak-*P* stages (Fig. 2A).

Warm Subduction

The *P*–*T* conditions of the Sanbagawa metamorphism have traditionally been classified as typifying high-*P* intermediate metamorphism (Miyashiro 1961), showing intermediate *P*/*T* gradients between high- and medium-*P*/*T* types. This definition is based on the mineralogical features: widespread occurrence of calcic and sodic–calcic amphiboles (actinolite, winchite, and barroisite; where such amphiboles in mafic rocks indicate lower *P*/*T* gradients than the blueschist facies), and the scarcity of high-*P*/*T* indicators such as jadeite + quartz. However, recognition of the regional eclogite-facies metamorphism in the belt challenged the traditional concept of metamorphic belts being characterized by constant *P*/*T* gradients. In the Eclogite unit, it is now clear that original high-*P* minerals have been mostly erased by strong lower-*P* overprinting during exhumation, and are preserved only in domains shielded from later-stage deformation or, microscopically, as inclusions in garnet (e.g., Ota et al. 2004; Taguchi et al. 2019). Selection and compilation of such original (peak-*P*) metamorphic conditions for the Shirataki and Eclogite units have enabled us to reconstruct the thermal structure along the Cretaceous subduction interface, which describes a sigmoidal curve in *P*–*T* space (Fig. 3A).

Mafic rocks (meta-basalt) show changes in their constituent minerals—and, hence, also their rock names—for different *P*–*T* conditions. In the Shirataki unit, the rock names vary from greenschist, via low-*P* blueschist (Fig. 3B), to epidote amphibolite (Fig. 3C), defining a relatively low *P*/*T* gradient at shallow levels (0.5 GPa/300 °C to 1.0 GPa/500 °C; Fig. 3A). These *P*–*T* conditions require relatively "warm" subduction, which may be due to, for example, subduction of a very young slab (down-going plate) or subduction associated with strong shear heating along the plate interface. In contrast, in the Eclogite unit, rarely preserved garnet + omphacite, the representative mineral assemblage of eclogite (Fig. 3D), indicates much deeper *P*–*T* conditions, ranging from the lawsonite/epidote transition to its higher-*T* side (1.7 GPa/500 °C to 2.4 GPa/700 °C; Fig. 3A). The nearly isothermal medium-*P* part (1.0–1.7 GPa) of the *P*–*T* curve is inferred from steep subduction *P*–*T* paths of glaucophane-rich eclogite in eastern Shikoku, recognized by the barroisite-to-glaucophane transition (Fig. 3A; e.g., Weller et al. 2015). The deepest record in the Eclogite unit (~80 km) coincides with the common coupling depth of the slab–mantle interface in modern subduction zones, and the associated relatively high-*T* conditions in the Iratsu bodies (650–750 °C) imply that their subducted positions were closer to the circulating hot mantle wedge (Fig. 4A; Aoya and Endo 2017).

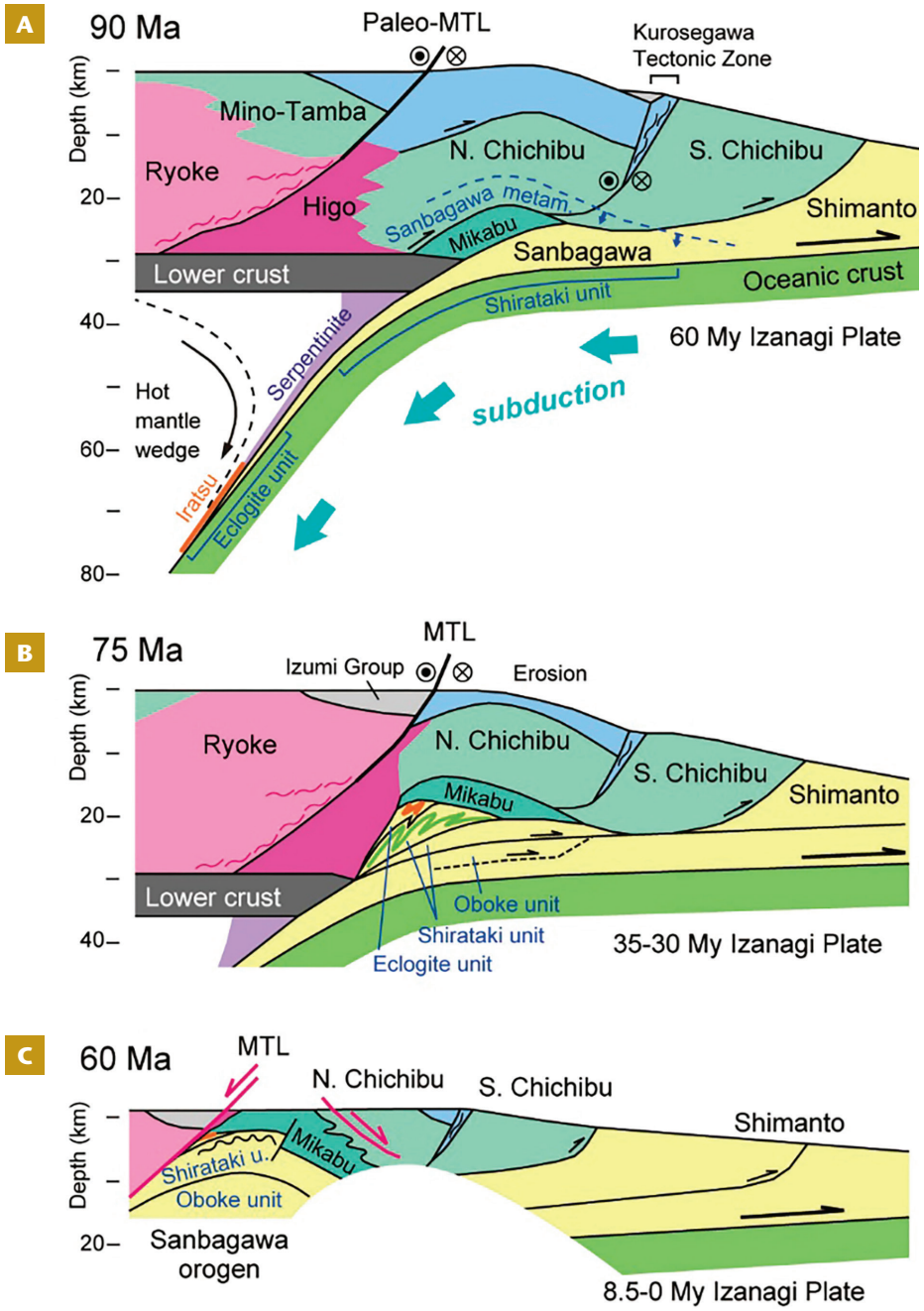

Figure 4 Schematic illustration showing subduction and exhumation of the Sanbagawa metamorphic rocks. Color scheme is the same as the legend of Figure 1A. Circular symbols indicate left-lateral displacement along the major faults. (**A**) The Shirataki and Eclogite units formed along the subduction interface (20–80 km depth). (**B**) Nappe stacking and orogen-subparallel extension (stretching direction perpendicular to this cross section) of the Sanbagawa metamorphic rocks. The Oboke unit was underplated during this period. (**C**) Normal faulting at the rear side of the shallow accretionary wedge.

BACK TO THE SURFACE

The Sanbagawa belt preserves an accumulated rock record of how the orogen has developed through time. Deep-seated rocks once present along the Cretaceous subduction interface at depths of 20–80 km are now concentrated within the Eclogite and Shirataki units, while the overlying accretionary wedge, which was already present at the time of subduction, is now preserved as the adjacent Chichibu belt. The reconstructed tectonic architecture (Fig. 4A) can account for the fact that part of the Chichibu belt was affected by the Cretaceous Sanbagawa metamorphism (Endo and Wallis 2017). The overall exhumation of the Sanbagawa belt seems to have been achieved in three steps, each with a distinct exhumation mechanism: buoyancy-driven upflow, ductile thinning, and, finally, a combination of normal faulting and erosion. The deepest process is recorded in the juxtaposition of the Eclogite unit (55–80 km depth) with the Shirataki unit (30–45 km depth), and is attributable to buoyancy-driven flow, which can also be loosely referred to as extrusion (Endo et al. 2012). Possible triggers for the onset of exhumation include: (1) subduction of large amounts of low-density sediments (Fig. 1B), (2) a decrease in the effective viscosity of the slab surface and interface domain due to an increase in temperature (Fig. 3A), and (3) the metasomatic formation of a weak talc-rich layer in the overlying mantle, which can act as a lubricant (Aoya and Endo 2017). The initial exhumation was completed in the time period 89–85 Ma (Wallis et al. 2009). Subsequently, the Eclogite and Shirataki units underwent tight folding and regional ductile deformation that involved orogen-subparallel extension (Fig. 4B), reflecting the contemporaneous oblique subduction of the Izanagi plate. The same oblique convergence is reflected in left-lateral displacement along the backstop, the paleo-MTL (Wallis et al. 2009; Aoya 2022). The high-strain ductile deformation associated with orogen-parallel stretching formed the main schistosity and stretching lineation throughout the Sanbagawa belt, and is the cause of the vertical thinning that caused exhumation up to mid-crustal levels (Wallis 1995).

Exhumation processes at the shallowest levels are dominated by brittle normal faulting and erosion. Underplating of additional tectonic units and upright folding after the main ductile deformation can be related to a new phase of crustal thickening, and this may have led to gravitational instability of the whole accretionary wedge (Aoya 2022). This thickening could be related to the approach and subduction of the Izanagi-Pacific ridge and triggered extensional collapse of the wedge (Kubota et al. 2020). This extension is shown by north-dipping normal faulting along the MTL (Kubota et al. 2020), pervasive normal faults in the Shirataki unit (Fukunari and Wallis 2007), and south-dipping normal faulting in the Northern Chichibu belt (Endo and Wallis 2017). This widespread normal faulting contributed to exhumation of the Sanbagawa belt above the brittle-ductile transition (Fig. 4C). Kubota et al. (2020) suggests the age of the normal faulting on the MTL was ~59 Ma. The Shirataki unit is non-conformably overlain by the Eocene shallow marine deposits (Kusuhashi et al. 2022; Fig. 1A), indicating that the Sanbagawa belt was exposed at the Earth's surface by ~46 Ma.

FUTURE DIRECTIONS

The semi-continuous internal structures of the Sanbagawa belt represent an excellent analogue of modern warm-subduction interface domains, such as SW Japan and Cascadia, specifically for depths ranging from the seismic/aseismic transition zone (~20–30 km) to the onset of strong slab–mantle coupling (~80 km). The rheological properties of these subduction interface domains remain poorly understood. The Sanbagawa belt has a range of rock types with microstructures and mineral assemblages suitable to extract further information from the rock records, through the application and development of various micro-gauges (e.g., temperature, pressure, stress, strain), as has been previously accomplished with Raman geothermobarometry. The structural architecture and exhumation processes of the Sanbagawa belt described in this chapter are supported by observations, but their viability should be further tested using numerical simulations incorporating geologically constrained boundary conditions and a reasonable range of physical parameters. Feedback from these simulations will aid in interpreting geological and geophysical data related to subduction interface processes, both modern and ancient.

ACKNOWLEDGMENTS

We thank the guest editors, Simon Wallis, Kazuhiro Miyazaki, and Ulrich Knittel for their invitation to write this article. Reviews by Atsushi Okamoto, Tetsuya Tokiwa, and Simon Wallis significantly improved this manuscript. This work is in part supported by JSPS KAKENHI grant numbers JP21H01188 and 21K03724.

REFERENCES

Angel RJ, Mazzucchelli ML, Alvaro M, Nestola F (2017) EosFit-Pinc: a simple GUI for host-inclusion elastic thermobarometry. American Mineralogist 102: 1957-1960, doi: 10.2138/am-2017-6190

Aoya M and 8 coauthors (2013) Geology of the Niihama District. Quadrangle Series, 1:50,000, Geological Survey of Japan (AIST), Tsukuba

Aoya M and Endo S (2017) Recognition of the 'early' Sambagawa metamorphism and a schematic cross-section of the Late-Cretaceous Sambagawa subduction zone. The Journal of the Geological Society of Japan 123: 677-698

Aoya M (2022) Overprint of secondary Du folding in the Sambagawa metamorphic belt, SW Japan: implications for strain ellipsoids and Paleogene tectonics of the east-Eurasian margin. Island Arc 31: e12463, doi: 10.1111/iar.12463

Endo S, Wallis SR, Tsuboi M, Aoya M, Uehara S-I (2012) Slow subduction and buoyant exhumation of the Sanbagawa eclogite. Lithos 146-147: 183-201, doi: 10.1016/j.lithos.2012.05.010

Endo S, Wallis SR (2017) Structural architecture and low-grade metamorphism of the Mikabu-Northern Chichibu accretionary wedge, SW Japan. Journal of Metamorphic Geology 35: 695-716, doi: 10.1111/jmg.12251

Endo S, Miyazaki K, Danhara T, Iwano H, Hirata T (2018) Progressive changes in lithological association of the Sanbagawa metamorphic complex, southwest Japan: relict clinopyroxene and detrital zircon perspectives. Island Arc 27: e12261, doi: 10.1111/iar.12261

Endo S, Yokoyama S (2019) Geology of the Motoyama District. Quadrangle Series, 1:50,000, Geological Survey of Japan (AIST), Tsukuba

Fukunari T, Wallis SR (2007) Structural evidence for large-scale top-to-the-north normal displacement along the Median Tectonic Line in southwest Japan. Island Arc 16: 243-261, doi: 10.1111/j.1440-1738.2007.00570.x

Hara H and 8 coauthors (2017) Detrital zircon multi-chronology, provenance, and low-grade metamorphism of the Cretaceous Shimanto accretionary complex, eastern Shikoku, southwest Japan: tectonic evolution in response to igneous activity within a subduction zone. Island Arc 26: e122128, doi: 10.1111/iar.12218

Hara H and 6 coauthors (2018) Geological Map of Japan 1:200,000, Kochi (2nd edition). Geological Survey of Japan (AIST), Tsukuba

Higashino T (1990) The higher grade metamorphic zonation of the Sambagawa metamorphic belt in central Shikoku, Japan. Journal of Metamorphic Geology 8: 413-423, doi: 10.1111/j.1525-1314.1990.tb00628.x

Kaneki S, Kouketsu Y (2022) An automatic peak deconvolution method for Raman spectra of terrestrial carbonaceous material for application to the geothermometers of Kouketsu et al. (2014). Island Arc 31: e12467, doi: 10.1111/iar.12467

Kouketsu Y, Nishiyama T, Ikeda T, Enami M (2014a) Evaluation of residual pressure in an inclusion–host system using negative frequency shift of quartz Raman spectra. American Mineralogist 99: 433-442, doi: 10.2138/am.2014.4427

Kouketsu Y, Enami M, Mouri T, Okamura M, Sakurai T (2014b) Composite metamorphic history recorded in garnet porphyroblasts of Sambagawa metasediments in the Besshi region, central Shikoku, southwest Japan. Island Arc 23: 263-280, doi: 10.1111/iar.12075

Kouketsu Y and 8 coauthors (2021) Thermal structure in subducted units from continental Moho depths in a palaeo subduction zone, the Asemigawa region of the Sanbagawa metamorphic belt, SW Japan. Journal of Metamorphic Geology 39: 727-749, doi: 10.1111/jmg.12584

Kubota Y, Takeshita T, Yagi K, Itaya T (2020) Kinematic analyses and radiometric dating of the large-scale paleogene two-phase faulting along the median tectonic line, southwest Japan. Tectonics 39: e2018TC005372, doi: 10.1029/2018TC005372

Kusuhashi N and 6 coauthors (2022) The Eocene Hiwadatoge Formation, SW Japan: constraints on the timing of the denudation of the Sambagawa metamorphic rocks. The Journal of the Geological Society of Japan 128: 411-426

Miyashiro A (1961) Evolution of metamorphic belts. Journal of Petrology 2: 277-311, doi: 10.1093/petrology/2.3.277

Miyazaki K and 10 coauthors (2016) Geological map of Japan 1:200,000, Matsuyama (2nd edition). Geological Survey of Japan (AIST), Tsukuba

Nagata M and 9 coauthors (2019) Timescale of material circulation in subduction zone: U–Pb zircon and K–Ar phengite double-dating of the Sanbagawa metamorphic complex in the Ikeda district, central Shikoku, southwest Japan. Island Arc 28: e12306, doi: 10.1111/iar.12306

Nozaki T, Kato Y, Suzuki K (2013) Late Jurassic ocean anoxic event: evidence from voluminous sulphide deposition and preservation in the Panthalassa. Scientific Reports 3: 1889, doi: 10.1038/srep01889

Ota T, Terabayashi M, Katayama I (2004) Thermobaric structure and metamorphic evolution of the Iratsu eclogite body in the Sanbagawa belt, central Shikoku, Japan. Lithos 73: 95-126, doi: 10.1016/j.lithos.2004.01.001

Taguchi T, Endo S, Igami Y, Miyake A (2019) A new occurrence of retrogressed eclogite from the Sanbagawa belt of southwest Japan and its significance. Island Arc 28: e12317, doi: 10.1111/iar.12317

Ueda H, Miyashita S (2005) Tectonic accretion of a subducted intraoceanic remnant arc in Cretaceous Hokkaido, Japan, and implications for evolution of the Pacific northwest. Island Arc 14: 582-598, doi: 10.1111/j.1440-1738.2005.00486.x

Wallis S (1995) Vorticity analysis and recognition of ductile extension in the Sanbagawa belt, SW Japan. Journal of Structural Geology 17: 1077-1093, doi: 10.1016/0191-8141(95)00005-X

Wallis SR and 6 coauthors (2009) Plate movements, ductile deformation and geochronology of the Sanbagawa belt, SW Japan: tectonic significance of 89–88 Ma Lu–Hf eclogite ages. Journal of Metamorphic Geology 27: 93-105, doi: 10.1111/j.1525-1314.2008.00806.x

Wallis SR, Okudaira T (2016) Paired metamorphic belts of SW Japan: the geology of the Sanbagawa and Ryoke metamorphic belts and the Median Tectonic Line. In: Moreno T, Wallis S, Kojima T, Gibbons W (eds) The Geology of Japan. The Geological Society of London, pp 101-124, doi: 10.1144/GOJ.4

Weller OM, Wallis SR, Aoya M, Nagaya T (2015) Phase equilibria modelling of blueschist and eclogite from the Sanbagawa metamorphic belt of southwest Japan reveals along-strike consistency in tectonothermal architecture. Journal of Metamorphic Geology 33: 579-596, doi: 10.1111/jmg.12134

Wu J, Lin Y-A, Flament N, Wu JT-J, Liu Y (2022) Northwest Pacific-Izanagi plate tectonics since Cretaceous times from western Pacific mantle structure. Earth and Planetary Science Letters 583: 117445, doi: 10.1016/j.epsl.2022.117445